Journal of Power Sources 395 (2018) 280–288

Contents lists available at ScienceDirect

Journal of Power Sources

journal homepage: www.elsevier.com/locate/jpowsour

Low-complexity online estimation for $LiFePO_4$ battery state of charge in electric vehicles

Jinhao Meng[a], Mattia Ricco[b], Anirudh Budnar Acharya[c], Guangzhao Luo[a,*], Maciej Swierczynski[d], Daniel-Ioan Stroe[b], Remus Teodorescu[b]

[a] School of Automation, Northwestern Polytechnical University (NPU), Xi'an, 710072, China
[b] Department of Energy Technology, Aalborg University, Aalborg, 9220, Denmark
[c] Department of Electric Power Engineering, Norwegian University of Science and Technology, Trondheim, 7491, Norway
[d] Lithium Balance A/S, Smørum, 2765, Denmark

HIGHLIGHTS

- Battery SOC is estimated with a low-complexity online method.
- Errors in the battery two RC equivalent circuit model are analyzed.
- Two PI filters are designed to compensate the errors in the battery model.
- An adaptively adjusted process is proposed to form the fusing weights of the PI filters.
- The execution time of the algorithms is measured on the MicroZed development board.

ARTICLE INFO

Keywords:
State of charge
$LiFePO_4$ battery
Online estimation
Low-complexity

ABSTRACT

This paper proposes a low-complexity online state of charge estimation method for $LiFePO_4$ battery in electrical vehicles. The proposed method is able to achieve accurate state of charge with less computational efforts in comparison with the nonlinear Kalman filters, and also can provide state of health information for battery management system. According to the error analysis of equivalent circuit model with two resistance and capacitance, two proportional-integral filters are designed to compensate the errors from inaccurate state of charge and current measurements, respectively. An error dividing process is proposed to tune the contribution of each filter to the finial estimation results, which enhances the validation and accuracy of the proposed method. Recursive least squares filter can provide the state of health information and updates the parameters of battery model online to eliminate the errors caused by parameters uncertainty. The proposed method is compared with extend Kalman filter in regards to accuracy and execution time. The execution time of the proposed method is measured on Zynq board platform to validate its suitability for online implementation. In this paper, the proposed method is able to obtain less than 1% error for state of charge estimation.

1. Introduction

Global warming triggering by the excessive emissions of the greenhouse gas not only breaks the balance of ecosystem but also threatens the survival of humanity. EVs are zero emission, which contain electrical motors providing propulsion and battery as the energy supply [1,2]. Li-ion batteries have many advantages, such as higher energy density, longer lifespan, and lower self-discharge rate [3,4]. The cost of Li-ion batteries in EVs has already declined around 14% annually from 2007 to 2014 and this trend seems to be maintained in the near future [5]. The superior characteristics of Li-ion technology and their respective price drop have made it popular as the power source in EVs. When battery pack acts as the fuel tank of the vehicle, SOC of the battery is the fuel gauge. More than a crucial parameter for EV drivers, SOC is also a key index in BMS [6,7]. In order to provide enough power and energy for automotive propulsion, hundreds (even thousands) of Li-ion batteries are connected in series or parallel. However, the discrepancy in each battery coming from the manufacturing tolerances causes a difference in SOC (even during the same charging or discharging process) [8]. BMS has to control the current flow between cells on the foundation of an accurate SOC. Otherwise, overcharge or over discharge will inevitably damage the battery's inner characteristics [9],

* Corresponding author.
E-mail address: guangzhao.luo@nwpu.edu.cn (G. Luo).

https://doi.org/10.1016/j.jpowsour.2018.05.082
Received 12 March 2018; Received in revised form 10 May 2018; Accepted 25 May 2018

shorten its lifespan, and even increase the risk of explosion [10].

SOC estimation methods available in the literature are mainly divided into four categories: Coulomb counting method [11,12], OCV method [13,14], model-based methods [15–18] and data-driven methods [19–21]. The necessity of an accurate initial SOC and the accumulation of the current measurement errors make the Coulomb counting method doubtful for a highly accurate SOC [22,23]. In order to measure an accurate OCV, a long relaxation time is needed to reach the battery's inner equilibrium condition [14]. Therefore, although OCV has a monotonous relationship with SOC, it is not suitable for online estimation. Data-driven SOC estimation utilizes machine learning algorithms [21]. However, collecting enough training data in real applications before usage is difficult. The robustness of data-driven methods under various working conditions is also not guaranteed. Model-based methods have advantages of being insensitive to initial SOC, which seems to be a better tradeoff between accuracy and computing efficiency. Accordingly, Kalman filter [16,18,24], H-infinity filter [25], and particle filter [26] are widely used to estimate SOC on the basis of the model-based structure. With the complexly computing process, these methods obtain relatively good results in SOC estimation.

The only way to know the battery SOC in real applications is the estimation from other measurements (such as current, voltage, etc) [27]. In EV, SOC of hundreds (or thousands) cells should be estimated online. Since the platforms for implementing the estimation algorithms are generally low cost microcontrollers, the computational power and resource are usually limited [28]. Therefore, accurate online SOC with less computational burden is a huge challenge for BMSs. In addition, the existing highly SOC methods mostly rely on complex calculation process [29–31]. For these reasons, this paper focuses on the online implementation of a low-complexity estimation method. PI observers have already been applied to estimate SOC in Refs. [28,32,33]. Xu et al. use in Ref. [32] a PI observer and one RC ECM for SOC estimation. However, the linearization of OCV-SOC brings errors to the estimation, and one RC model is also limited in describing the dynamic behavior of Li-ion battery. Two PI controllers are applied in Refs. [28] and [33] for SOC estimation. A mathematical model is used in Ref. [33] without parameter update, which limits the modeling accuracy, especially under dynamic driving cycles. This estimation method relies on a weight function containing four parameters to guarantee its accuracy in the quasi-unobservable regions, which also means a more complex trial and error process is needed for tuning those parameters. In Ref. [28], the SOC and SOH are simultaneously estimated by means of a parameter-varying circuit model. The SOC estimation structure totally relies on the OCV, which limits its usage on the type of battery that have a relatively flat OCV-SOC curve. An on-line implementable SOC is proposed for a System-on-Chip device in this paper. Better accuracy and faster execution time in comparison with the EKF are achieved.

Different from the previous works, this paper designs a low-complexity model-based structure for SOC estimation by analyzing the errors of the two RC ECM and adaptively dividing the deviation. In the proposed estimation structure, the errors from inaccurate initial SOC and current measurement are compensated by two PI filters. However, according to the benefits of each PI filter on modeling accuracy, errors between the output of the battery model and the terminal voltage are split into two parts by an adaptively adjusted process. The output of the PI filters is then substituted into the Coulomb counting function for SOC estimation. For the purpose of acquiring SOH information and avoiding parameters uncertainty simultaneously, parameters of the two RC elements are identified online by RLS. Compared with EKF, the benefits of the proposed model-based structure are good accuracy in SOC estimation and lower computation burden. These improvements are proved through experimental results.

This paper is organized as follows. Section 2 describes the modeling process and analyzes the sources of modeling error. The proposed model based SOC estimator including two designed PI filters and a weight adaptively adjusted process is presented in Section 3.

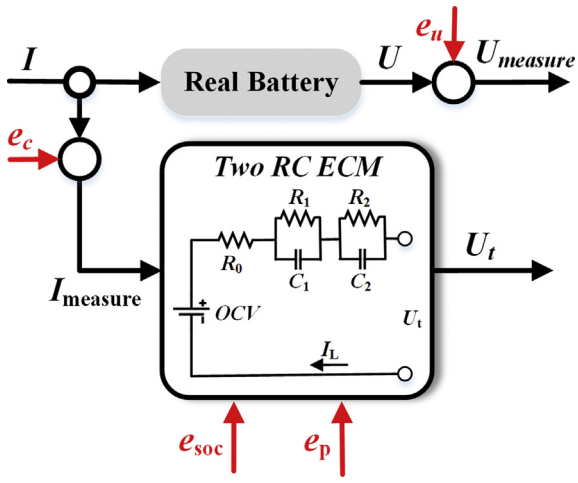

Fig. 1. Error sources of the two RC ECM.

Experimental tests on the accuracy and execution time are shown in Section 4. Conclusions are given in Section 5.

2. Battery model and error analysis

ECMs are popular in the battery SOC estimation field, and each circuit component in the ECM usually has a physical-chemical meaning.

2.1. Two RC battery ECM

As shown in Fig. 1, a two RC ECM consists of an internal resistance, two additional RC networks, and one ideal voltage source. The two different RC networks contain the long time constant related to the diffusion process in the electrolyte and porous electrodes, and the short time constant indicating the charge transfer and the double-layer effect in the electrode. The two RC ECM has proven to be a good tradeoff between the computing complexity and the accuracy in modeling the dynamic behavior of Li-ion batteries [34]. Therefore, this paper selects the ECM with two RC networks modeling the battery static and dynamic performance.

According to the Kirchhoff's circuit laws, the two RC ECM as illustrated in Fig. 1 is expressed as follows:

$$U_t = OCV - U_1 - U_2 - I_L \cdot R_0 \tag{1}$$

$$I_L = \frac{U_1}{R_1} + C_1 \frac{dU_1}{dt} = \frac{U_2}{R_2} + C_2 \frac{dU_2}{dt} \tag{2}$$

where R_0 is the ohmic resistance, U_1 is the voltage of the first RC pair and U_2 is the voltage of the second RC pair.

OCV has a monotonous relationship with SOC, which can be simply expressed as Eq. (3).

$$OCV = f(SOC) \tag{3}$$

From Eqs. (1)–(3), it is easy to find out that the terminal voltage U_t is related to SOC, current, and RC parameters. The transfer function of the two RC model is:

$$U_t = f(SOC) - \left(\frac{R_1}{1 + R_1 \cdot C_1 \cdot s} + \frac{R_2}{1 + R_2 \cdot C_2 \cdot s} + R_0 \right) \cdot I_L \tag{4}$$

2.2. Error analysis of the two RC ECM

It can be seen from Eq. (4) that inaccurate SOC, current measurement error, and RC parameters uncertainty definitely bring errors to the model output. The error in OCV is hard to avoid because of the inaccurate initial SOC. Furthermore, the RC parameters change with the

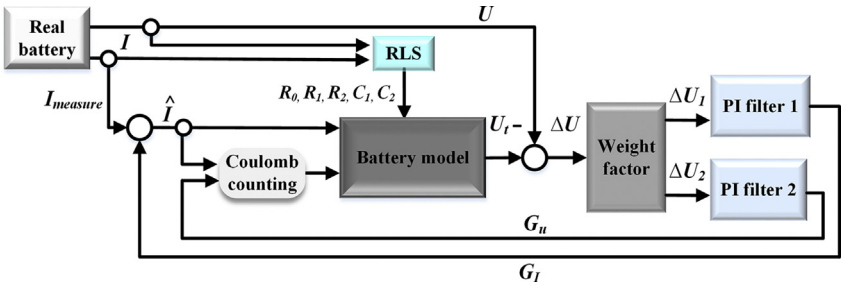

Fig. 2. Framework of the proposed method.

chemical reactions inside the battery.

Fig. 1 presents the error sources on the basis of the previous analysis. In Fig. 1, errors from inaccurate SOC are defined as e_{soc}, errors from the current sensor are e_c, errors from the voltage sensor are e_u, and errors from parameter uncertainty are e_p. The deviation between the output of the battery model and the voltage measurement acts as the new information for correcting SOC in the model-based estimation.

3. Low-complexity online SOC estimation

Generally, the current measurement error comes from several specific aspects. The current measurement contains the true current, the random noise, the measurement bias, and the nonlinearity errors. In addition, self-discharge and the current loss of power electronics also reduce the accuracy of the current measurement [35]. The exact value of each error is not known, but the random errors with zero mean can be eliminated in the SOC calculation process because of the integration of the current. Unfortunately, not all of the above mentioned errors are zero mean. Thus, the first PI filter should be designed to compensate for the current measurement error.

ΔU is defined as the difference between the output of battery model and the terminal voltage. ΔU coming from the current measurement is ΔU_1 and from the inaccurate SOC is ΔU_2. Errors from parameters uncertainty ΔU_3 are temporary ignored, which will be discussed later in this paper. The modeling error is expressed as:

$$\Delta U = \Delta U_1 + \Delta U_2 = U_{measure} - U_t = U_{measure} - (OCV - U_1 - U_2 - I_L \cdot R_0) \tag{5}$$

3.1. The design of the two PI filters

The first PI filter is designed to eliminate the current measurement error ΔU_1. The expression of the first PI filter is [33]:

$$G_I = K_{p,I} \cdot \left(\Delta U_1 + \frac{1}{T_{i,I}} \cdot \sum_{i=0}^{k} \Delta U_1 \right) \tag{6}$$

where $K_{p,I}$ is the proportional gain and $1/T_{i,I}$ is the integration gain.

The input current of the battery model $\hat{I}$ is corrected by the gain of the PI filter G_I:

$$\hat{I} = I_{measure} + G_I \tag{7}$$

Afterward, $\hat{I}$ is feedback to the Coulomb counting function as following:

$$SOC_i(k+1) = SOC(k) - \frac{\eta \cdot T}{C_n} \cdot \hat{I}(k+1) \tag{8}$$

The second PI filter is established for reducing ΔU_2. The expression of this PI filter is as follows:

$$G_U = K_{p,U} \cdot \left(\Delta U_2 + \frac{1}{T_{i,U}} \cdot \sum_{i=0}^{k} \Delta U_2 \right) \tag{9}$$

where $K_{p,U}$ is also the proportional gain and $1/T_{i,U}$ is the integration gain.

Since the only relationship between SOC and the output of the battery model is the term f (SOC), G_U is directly added to Coulomb counting function in Eq. (10).

$$SOC(k+1) = SOC_i(k+1) + G_U \tag{10}$$

Substituting Eq. (8) into Eq. (10), Eq. (11) is obtained as:

$$SOC(k+1) = SOC(k) - \frac{\eta \cdot T}{C_n} \cdot \hat{I}(k+1) + G_U \tag{11}$$

Considering the fact that accurate initial SOC is hard to know in advance in most applications, the gains should be larger at the primary stage of the proposed method and then quickly decreases after certain estimation steps. In this paper, the updated coefficient is designed in form of Eq. (12).

$$K_A = a \cdot e^{-b \cdot t} + 1 \tag{12}$$

Then, considering the coefficient in Eq. (12), the SOC estimation method is expressed as:

$$SOC(k+1) = SOC(k) - \frac{\eta \cdot T}{C_n} \cdot \hat{I}(k+1) + K_A \cdot G_U \tag{13}$$

3.2. The framework of the proposed SOC estimation method

Fig. 2 clearly indicates the entire structure of the proposed method. The adopted battery model is the two RC ECM whose parameters are updated online through RLS parametric identification method. The difference between the measured voltage and the output of battery model is divided into two parts that derive from the current measurement errors and the inaccurate SOC estimation. According to the two sources of errors, the two PI filters are designed to improve the accuracy of the battery model. The outputs of the two PI filters compensate the estimated SOC, which decreases the effects of inaccurate SOC and current measurement error in the traditional Coulomb counting method. Since PI filter, ECM, and RLS are effective methods for industry applications, SOC is possible to be estimated with low-complexity. Section 4.2 will show the computational complexity of the proposed structure in more details.

Different from other structures with two PI filters, this paper automatically divides the voltage error into two parts as shown in the weight factor part of Fig. 2. The goal of the two PI filters is to remove the errors related to current measurement and SOC uncertainty. Thanks to this filtering, the proposed method can estimate accurately the battery SOC. The error between the battery model and the voltage measurement is adopted for updating the weight factors online.

According to the sources of the errors, we define that:

$$\Delta U_1 = p_1 \cdot \Delta U \tag{14}$$

$$\Delta U_2 = p_2 \cdot \Delta U \tag{15}$$

Where ΔU, ΔU_1 and ΔU_2 are the same as previously described, p_1 and p_2 are the weight factors. Due to the nonlinearity of battery inner characteristics, p_1 and p_2 are assigned to specify initial values. Afterwards, they are updated online during the entire estimation for ensuring the

accuracy of SOC. The updating mechanism of weight factor is detailed as the following steps:

***Step* 1**. Assuming ΔU is the input of the first PI filter, the output of the battery model U_a is obtained;
***Step* 2**. Assuming ΔU is the input of the second PI filter, the output of the battery model U_b is obtained;
***Step* 3**. Weight factors are calculated as:

$$p_1 = \frac{|U - U_b|}{|U - U_a| + |U - U_b|} \tag{16}$$

$$p_2 = \frac{|U - U_a|}{|U - U_a| + |U - U_b|} \tag{17}$$

p_1 and p_2 are actually fused the results of the two PI filters. When SOC and current measurement are accurate, the output of the battery model is supposed to be equal to the voltage measurement. Therefore, Eqs. (16) and (17) can be seen as the measurement of how accurate SOC we can get if one PI filter is selected.

3.3. The online parameter identification in the proposed method

In Fig. 2, it is also illustrated that the parameters are updated online for eliminating the parameter uncertainty. The battery works at various driving cycles, which means the parameters of the battery model keep changing in real-time applications. The identifiability of the nth-order battery ECM has been proven in Ref. [36]. The RLS technique can recursively minimize the cost function, which is popular in the area of parameter identification for its excellent performance [25,37]. Therefore, we select RLS to identify the parameters in this paper.

Derived from Eq. (4), the transfer function of the two RC model is:

$$G(s) = U_t(s) - OCV(s) = -\left(\frac{R_1}{1 + R_1 \cdot C_1 \cdot s} + \frac{R_2}{1 + R_2 \cdot C_2 \cdot s} + R_0\right) \cdot I(s) \tag{18}$$

In order to apply the transfer function to a digital system, it should be transformed from s domain to z domain. Bilinear transformation is used in this paper since it ensures the stability of the discrete system consistent with the continuous system. The expression of the bilinear transformation is:

$$s = \frac{2}{T}\frac{1 - z^{-1}}{1 + z^{-1}} \tag{19}$$

The discretized two RC model is:

$$G(z^{-1}) = \frac{b_3 + b_4 \cdot z^{-1} + b_5 \cdot z^{-2}}{1 - b_1 \cdot z^{-1} - b_2 \cdot z^{-2}} \tag{20}$$

where b_1, b_2, b_3, b_4, b_5 are the parameters to be identified from RLS.

The sampling time T is 1 s in this paper. Since the variation of SOC is very small in one sample time, OCV is regarded as a constant value during this period [38,39]. Eq. (21) is further used in RLS for parameter identification.

$$U(k) = b_1 \cdot U(k-1) + b_2 \cdot U(k-2) + b_3 \cdot I(k) + b_4 \cdot I(k-1) + b_5 \cdot I(k-2) + (1 - b_1 - b_2) \cdot OCV \tag{21}$$

Then, we define that:

$$\phi(k) = [U(k-1) \;\; U(k-2) \;\; I(k) \;\; I(k-1) \;\; I(k-2) \;\; 1],$$
$$\theta(k) = [b_1 \;\; b_2 \;\; b_3 \;\; b_4 \;\; b_5 \;\; (1 - b_1 - b_2) \cdot OCV],$$
$$y(k) = U(k).$$

In this paper, a modification of the normal RLS method is used by adding an additional forgetting factor to discount the historical input data [39]. The benefits of the forgetting factor are that it helps the RLS to discard gradually the past data and also guarantees the recent data can play a greater role in identifying the new parameters. The RLS recursive process including forgetting factor is as follows:

$$\hat{y}(k) = \phi^T(k)\theta(k-1) \tag{22}$$

$$\theta(k) = \theta(k-1) + K(k)(y(k) - \hat{y}(k)) \tag{23}$$

$$K(k) = q(k)\phi(k) \tag{24}$$

$$q(k) = \frac{P(k-1)}{\lambda + \phi^T(k)P(k-1)\phi(k)} \tag{25}$$

$$P(k) = \frac{1}{\lambda}\left(P(k-1) - \frac{P(k-1)\phi(k)\phi^T(k)P(k-1)}{\lambda + \phi^T(k)P(k-1)\phi(k)}\right) \tag{26}$$

Where λ is the forgetting factor, which typically is between 0.98 and 0.995 [40], $K(k)$ is the gain for parameter identification, $P(k)$ is the covariance matrix. The parameters b_1, b_2, b_3, b_4, b_5 in Eq. (21) are directly calculated from RLS. Afterward, the RC parameters are calculated from the following equations:

$$R_0 = -\frac{b_3 - b_4 + b_5}{b_1 - b_2 + 1} \tag{27}$$

$$R_1 \cdot C_1 \cdot R_2 \cdot C_2 = -\frac{T^2 \cdot (b_1 - b_2 + 1)}{4 \cdot (b_1 + b_2 - 1)} \tag{28}$$

$$R_1 \cdot C_1 + R_2 \cdot C_2 = -\frac{T \cdot (1 + b_2)}{b_1 + b_2 - 1} \tag{29}$$

$$R_0 + R_1 + R_2 = \frac{b_3 + b_4 + b_5}{b_1 + b_2 - 1} \tag{30}$$

$$R_1 \cdot C_1 \cdot (R_0 + R_2) + R_2 \cdot C_2 \cdot (R_0 + R_1) = \frac{T \cdot (b_3 - b_5)}{b_1 + b_2 - 1} \tag{31}$$

Internal resistance is increasing during the battery aging process [29,41]. Therefore, SOH information can also be obtained as follows [42]:

$$SOH = \frac{R_{0,EOL} - R_0}{R_{0,EOL} - R_{0,new}} \times 100\% \tag{32}$$

where $R_{0,EOL}$ is the internal resistance at the end of the battery lifespan, $R_{0,new}$ is the internal resistance of the new battery. Consequently, SOH information is able to be received from the proposed structure.

4. Experimental result

The test bench for collecting battery measurement consists of a host computer, a battery test station (MACCOR 4000 series), and a $LiFePO_4$ battery cell. The battery test station performs the charging and discharging profiles in the temperature chamber. The measurement is then sent to the host computer. The accuracy of the test bench is ± 0.01% + 1 digit for voltage measurement and ± 0.02% + 1 digit for current measurement. The 10Ah cylindrical $LiFePO_4$ battery is tested in MACCOR for validating the proposed method. Table 1 lists the parameters of the Li-ion battery from the manufacturer.

Table 1
Parameters of the $LiFePO_4$ battery from manufacturer.

Item	Rating
Nominal Capacity	10Ah
Nominal Voltage	3.2 V
Maximum Charge Current	3C
Maximum Discharge Current	10C
Maximum Voltage	3.65 V
Cut Off Voltage	2.0 V

4.1. The experimental validation

The OCV-SOC relationship is an important element in the two RC ECM. Because of the strong hysteresis effect of the voltage in $LiFePO_4$ battery [43], OCV in charge and discharge process is measured simultaneously. In order to reach the battery inner equilibrium, the OCV is measured after 2 h' rest in the chamber. The interval of OCV measurement is 5% SOC and the chamber temperature is constantly set to 25 °C. In this paper, we calculate the average OCV of charge and discharge condition for ensuring the accuracy of the curve fitting.

In order to guarantee the diminishing of OCV with the decrease of SOC, quadratic optimization is applied to solve the curve fitting problem [43]. High-order polynomial function in Eq. (33) represents the OCV-SOC relationship used in the experiment of this paper, and the mean absolute error between the average OCV and the curve fitting results is merely 0.0108 mV.

$$\begin{aligned} OCV = &-330.2741\cdot SOC^8 + 1507.8350\cdot SOC^7 - 2869.7023 \\ &\cdot SOC^6 + 2949.8632\cdot SOC^5 - 1773.9467\cdot SOC^4 + 632.0383 \\ &\cdot SOC^3 - 128.9882\cdot SOC^2 + 13.8940\cdot SOC + 2.6371 \end{aligned} \tag{33}$$

The NEDC [44] and UDDS [45] are adopted for validating the proposed method in dynamic driving cycles. It should be noted that the positive value of current means battery is in discharge condition and the negative value denotes the charge condition. The ambient temperature is set to 25 °C. A $LiFePO_4$ battery is firstly discharged under multi-cycle NEDC until it reaches the cut-off discharge voltage. The current and voltage are measured and recorded during the discharging process as shown in Fig. 3. We can see that the voltage changes dramatically when the energy left in the battery is close to zero. This indicates that the battery has a stronger nonlinearity behavior in the low SOC area. The black line in Fig. 3(b) is the voltage prediction of the two RC ECM, whose parameters are identified from RLS. The mean absolute error is 0.0012 V in Fig. 3(b), which indicates the accuracy of the parameter identification in NEDC.

EKF is quite popular in the area of states estimation, especially for the battery SOC estimation. Thereby, the proposed method is compared with EKF in terms of estimation accuracy and execution time. Due to the inaccurate initial SOC, in reality, the initial SOC in this experiment is arbitrarily set to 0.7. The experimental results of NEDC in Fig. 4(a) shows that the two methods can deal with inaccurate initial SOC. The

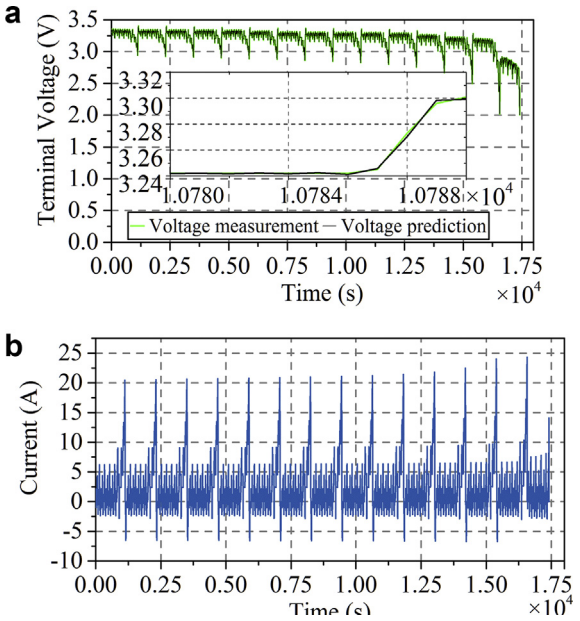

Fig. 3. Battery measurement in NEDC: (a) current; (b) terminal voltage.

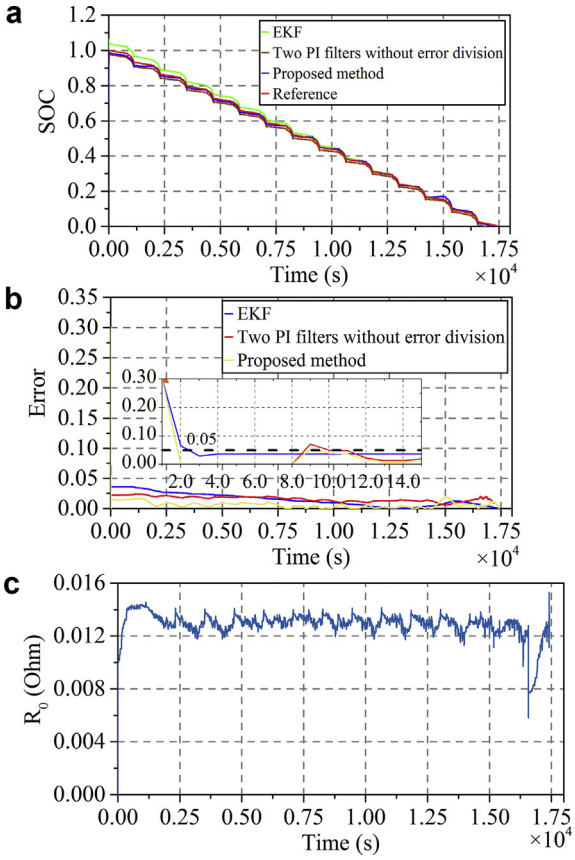

Fig. 4. Estimation results in NEDC: (a) SOC estimation; (b) absolute error of SOC estimation; (c) internal resistance estimation.

proposed method is able to track the reference SOC in 2 s, and EKF converges to the reference SOC in 3 s in Fig. 4(b). It also shows that the proposed method tracks faster and stays closer to the reference value. Indeed, the absolute error of the proposed method is lower than EKF in most conditions. The RMSE of the proposed method is 0.0062, while it is 0.0160 for two PI filters without error division. The RMSE is 0.0151 for EKF, and the RMSE of the proposed technique is almost half of EKF. The maximum absolute error is calculated after 15 s of SOC estimation in this paper. The maximum absolute error is 0.0364 for EKF. It is 0.0246 for two PI filters without error division and 0.0186 for the proposed method. Thus, this experiment proves the higher accuracy of the proposed method. Moreover, the estimated resistance in Fig. 4(c) can be further used as an indicator of the battery SOH information.

For further validating the proposed method, multicycle UDDS is also applied to the same battery under 25 °C. The details in Fig. 5(a) and Fig. 5(b) clearly show that UDDS is more severe in variation than NEDC. The predicted voltage with parameters from RLS is also shown as the black line in Fig. 5(b). The mean absolute error is 0.0025 V in UDDS, which proves the accuracy of the RLS estimation results.

The initial SOC is also set to 0.7. In Fig. 6, the estimation results of the proposed method track faster and keep closer to the real SOC in comparison with the EKF. RMSE of the proposed method in UDDS is 0.0077, while it is 0.0137 for two PI filters without error division. Moreover, the RMSE is 0.0147 for EKF. In UDDS, the maximum absolute error is 0.0319 for EKF after the 15 s of estimation. It is 0.0269 for two PI filters without error division and 0.0145 for the proposed method. Experimental results prove the accuracy of the proposed method. The internal resistance in Fig. 6(c) also indicates the battery SOH information. In the above two tests, the experimental results have sufficiently proven that the proposed method has good performance in the estimation accuracy.

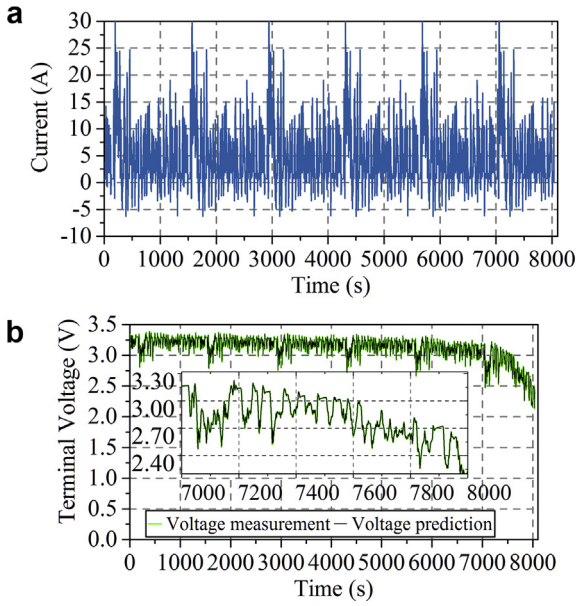

Fig. 5. Battery current and voltage measurement in UDDS: (a) current; (b) terminal voltage.

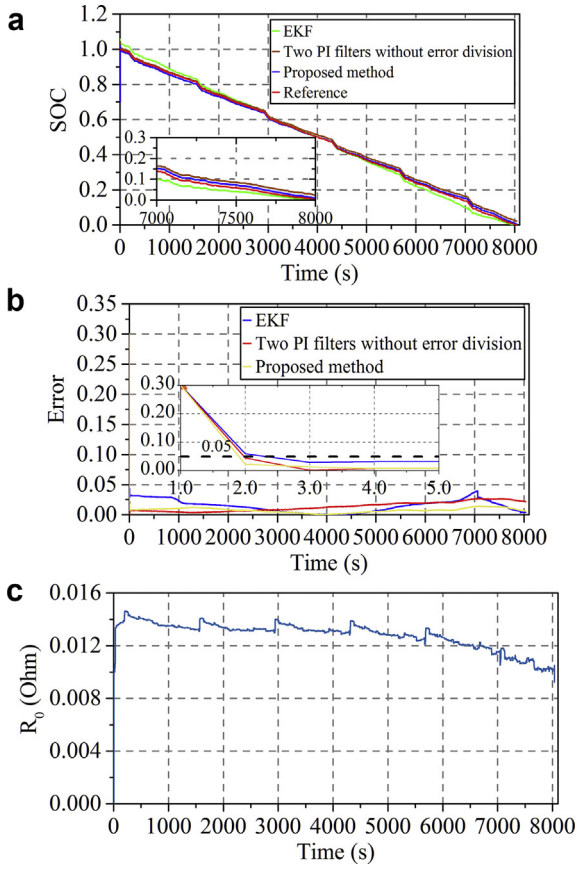

Fig. 6. Estimation results in UDDS: (a) SOC estimation; (b) absolute error of SOC estimation; (c) internal resistance estimation.

4.2. The execution time of the proposed method

For further investigation of the proposed method in terms of computational burden, the two above mentioned methods are executed in a MicroZed development board (Xilinx Zynq XC7Z020). The block diagram of the verification process is illustrated in Fig. 7. The proposed

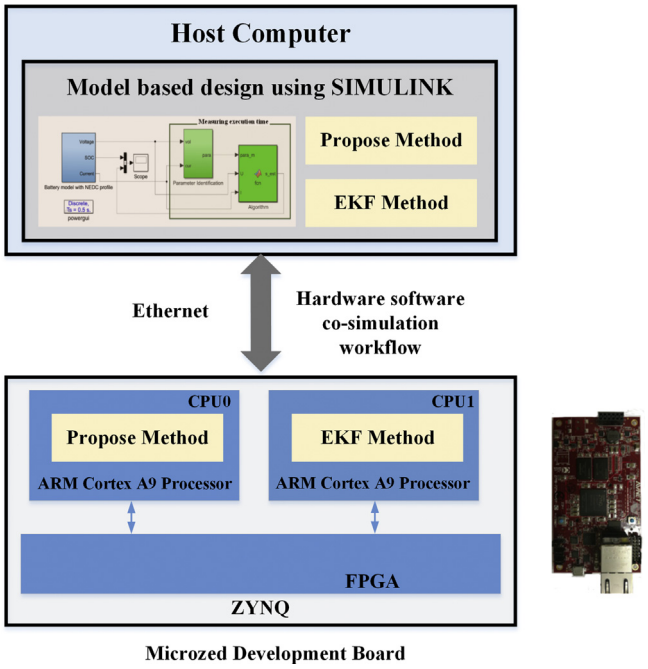

Fig. 7. The structure of the processor-in-the-loop test.

method and EKF are established in Simulink/MATLAB, and then directly downloaded to the ARM core in the Zynq through model-based design approach. The Simulink model used to measure the execution time contains the SOC estimation and the parameter identification method. After having run all the algorithms in a processor-in-the-loop way, their execution time has been evaluated. The average execution time of the EKF and the proposed method are 0.116716 ms and 0.035232 ms, respectively. It means that the proposed technique is 3.3 times faster than EKF in the Zynq processor. In the model-based design approach, the complexity of the proposed method is 3 and the complexity of EKF is 14 (The complexity of algorithm is detailed in Ref. [30].). Therefore, the experimental results have proven the greater performance in terms of computing efficiency and accuracy of the proposed method. Due to the lower execution time, the proposed algorithm can be used in most online applications.

5. Conclusion

Online SOC and SOH estimation methods with good accuracy are needed for the BMS. By analyzing the error of the widely used two RC battery model, a low-complexity online SOC estimation method is proposed in this paper. The error of the two RC model has three main sources: inaccurate SOC, current measurement error and parameter uncertainty. Hence, two PI filters are used for compensating the inaccurate SOC and the current measurement error, respectively. RLS decreases the parameters uncertainty and also estimates the internal resistance as a possible SOH indicator. The two weight factors proposed in the paper divide the voltage error into two parts through an adaptively adjusted process. The comparison in experimental tests has proven the benefits of the weight factors in improving the SOC estimation accuracy. The outputs of the two PI filters are utilized in the Coulomb counting function to estimate the final result. The proposed method has been compared with EKF in term of accuracy and execution time. RMSE of the proposed method in SOC estimation is lower than EKF at the same initial condition. The average execution time of the proposed method is 0.035232 ms, which is just 30% of the EKF. The complexity of the proposed method is also less than that of EKF. The experimental results have proven that the proposed method has better performance in both estimation accuracy and computing efficiency.

Thus, it is more suitable for solving online SOC estimation problem than EKF. Since aging test of the Li-ion battery needs a long time, more works are still needed on validating the SOH estimation of the proposed method in the future. Moreover, the validation of the proposed method on other Li-ion technologies is still needed for future research.

Acknowledgments

This work was supported in part by the Key Program for International S&T Cooperation and Exchange Projects of Shaanxi Province (Grant number 2017KW-ZD-05) and the Fundamental Research Funds for the Central Universities (Grant number 3102017JC06004) and (Grant number 3102017OQD029). Jinhao Meng would like to thank the China Scholarship Council for supporting his study in the Department of Energy Technology, Aalborg University.

Appendix A

According to the approach in Ref. [32], the observability and stability of the proposed method are shown as follows.

The following equations are directly obtained from two RC ECM.

$$U_t = h(x) = OCV - U_1 - U_2 - I_L \cdot R_0 \tag{A.1}$$

$$I_L = \frac{U_1}{R_1} + C_1 \cdot \frac{dU_1}{dt} = \frac{U_2}{R_2} + C_2 \cdot \frac{dU_2}{dt} \tag{A.2}$$

$$OCV = f(SOC) = a_1 \cdot SOC^8 + a_2 \cdot SOC^7 + a_3 \cdot SOC^6 + a_4 \cdot SOC^5 + a_5 \cdot SOC^4 + a_6 \cdot SOC^3 + a_7 \cdot SOC^2 + a_8 \cdot SOC + a_9 \tag{A.3}$$

Taylor's formula can linearize the nonlinear function $g(x)$ on an arbitrarily stable point x_e.

$$g(x) = g(x_e) + \frac{\partial g(x_e)}{\partial x_e} \cdot (x - x_e) + R_n(x, x_e) \tag{A.4}$$

where $\frac{\partial g(x_e)}{\partial x_e}$ is the Jacobian matrix at the equilibrium point x_e. If the higher order terms $R_n(x, x_e)$ in Eq. (A.4) are neglected, Eq. (A.5) is obtained.

$$g(x) = g(x_e) + \frac{\partial g(x_e)}{\partial x_e} \cdot (x - x_e) \tag{A.5}$$

The linearized method in Eq. (A.5) is applied to the battery model. We define the system states as $x = [U_1 \;\; U_2 \;\; SOC]^T$, the input and output are $u = I$ and $y = U$. Then, the battery model is linearized as following:

$$\begin{cases} \dot{\bar{x}} = A \cdot \bar{x} + B \cdot \bar{u} \\ \bar{y} = C \cdot \bar{x} + D \cdot \bar{u} \end{cases} \tag{A.6}$$

where $\bar{x} = x - x_e$, $\bar{u} = I - I_e$, $A = \begin{bmatrix} -\frac{1}{R_1 \cdot C_1} & 0 & 0 \\ 0 & -\frac{1}{R_2 \cdot C_2} & 0 \\ 0 & 0 & 0 \end{bmatrix}$, $B = \begin{bmatrix} \frac{1}{C_1} \\ \frac{1}{C_2} \\ \frac{\eta}{C_n} \end{bmatrix}$, $C = \begin{bmatrix} -1 \\ -1 \\ \frac{\partial f(SOC_e)}{\partial SOC_e} \end{bmatrix}$, $D = R_0$.

The observability of the battery model can be proven by the rank of the following matrix:

$$\begin{bmatrix} C \\ CA \\ CA^2 \end{bmatrix} = \begin{bmatrix} -1 & -1 & \frac{\partial f(SOC_e)}{\partial SOC_e} \\ \frac{1}{R_1 \cdot C_1} & \frac{1}{R_2 \cdot C_2} & 0 \\ -\frac{1}{R_1^2 \cdot C_1^2} & -\frac{1}{R_1^2 \cdot C_1^2} & 0 \end{bmatrix} \tag{A.7}$$

The function f(SOC) is constrained to continuously decrease with SOC. Hence, $\frac{\partial f(SOC_e)}{\partial SOC_e}$ will not be zero, the term $R_1 \cdot C_1$ and $R_2 \cdot C_2$ are also not zero. The observability matrix is always full rank. Therefore, it is possible to estimate the states of the Li-ion battery.

For the convenience of proving the stability, the structure of the PI filter (Fig. A1(a)) is transformed to another identical form (Fig. A1(b)).

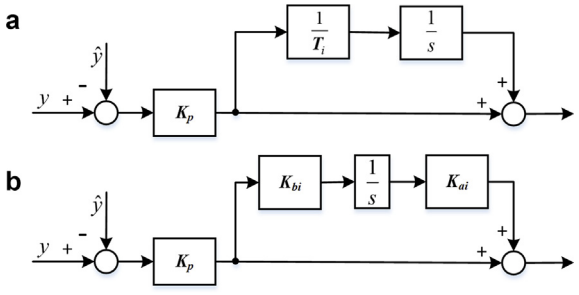

Fig. A.1. Structure of the PI filter: (a) the original structure; (b) the identical structure.

The PI filters in our paper are designed as following:

$$\begin{cases} \dot{\hat{x}} = A\cdot\hat{x} + B\cdot u + K_{p1}\cdot p_1\cdot(y-\hat{y}) + K_{p1}\cdot K_{a1i}\cdot p_1\cdot w_1 \\ +K_{p2}\cdot p_2\cdot(y-\hat{y}) + K_{p1}\cdot K_{a2i}\cdot p_2\cdot w_2 \\ \dot{w}_1 = K_{b1i}\cdot(y-\hat{y}) \\ \dot{w}_2 = K_{b2i}\cdot(y-\hat{y}) \end{cases} \tag{A.8}$$

We define $e = \hat{x} - x$. Then, the error between the battery model and the voltage measurement is defined as:

$$y - \hat{y} = C\cdot(x-\hat{x}) = -C\cdot e \tag{A.9}$$

Afterwards, Eq. (A.10) is obtained:

$$\begin{cases} \dot{e} = A\cdot e - K_{p1}\cdot C\cdot p_1\cdot e + K_{p1}\cdot K_{a1i}\cdot p_1\cdot w_1 \\ -K_{p2}\cdot C\cdot p_2\cdot e + K_{p2}\cdot K_{a2i}\cdot p_2\cdot w_2 \\ \dot{w}_1 = -K_{bi1}\cdot C\cdot e \\ \dot{w}_2 = -K_{bi2}\cdot C\cdot e \end{cases} \tag{A.10}$$

Eq. (A.10) can be changed to the following form:

$$\begin{pmatrix} \dot{e} \\ \dot{w}_1 \\ \dot{w} \end{pmatrix} = A_e\cdot\begin{pmatrix} e \\ w_1 \\ w_2 \end{pmatrix} \tag{A.11}$$

The matrix A_e is then as following:

$$A_e = \begin{bmatrix} A - K_{p1}\cdot p_1\cdot C - K_{p2}\cdot p_2\cdot C & K_{p1}\cdot K_{ai1}\cdot p_1 & K_{p2}\cdot K_{ai2}\cdot p_2 \\ -K_{bi1}\cdot p_1\cdot C & 0 & 0 \\ -K_{bi2}\cdot p_2\cdot C & 0 & 0 \end{bmatrix}$$

According to [46] and [47], the identified parameters θ_N converges to the expected value θ^* when $t\to\infty$. $\sqrt{N}\cdot(\theta_N - \theta^*)$ is bounded to a certain range in the normal distribution with zero mean and a specific covariance matrix. We define the error bound of the identified parameters as Δ and assume that the bound of A_e is A_e^*:

$$A_e = \begin{bmatrix} A + \Delta_{param} - K_{p1}\cdot p_1\cdot C - K_{p2}\cdot p_2\cdot C & K_{p1}\cdot K_{ai1}\cdot p_1 & K_{p2}\cdot K_{ai2}\cdot p_2 \\ -K_{bi1}\cdot p_1\cdot C & 0 & 0 \\ -K_{bi2}\cdot p_1\cdot C & 0 & 0 \end{bmatrix}$$

Since the observability of the system has been proven, the pole place method and LQ method can be used to design the PI gains and ensure the matrix A_e^* meets the requirement of the Hurwitz criterion. Therefore, the system will converge to the true states as $t\to\infty$.

References

[1] X. Hu, C. Zou, C. Zhang, Y. Li, Technological developments in batteries: a survey of principal roles, types, and management needs, IEEE Power Energy Mag. 15 (2017) 20–31, http://dx.doi.org/10.1109/MPE.2017.2708812.

[2] C.M. Martinez, X. Hu, D. Cao, E. Velenis, B. Gao, M. Wellers, Energy management in plug-in hybrid electric vehicles: recent progress and a connected vehicles perspective, IEEE Trans. Veh. Technol. 66 (2017) 4534–4549, http://dx.doi.org/10.1109/TVT.2016.2582721.

[3] B. Diouf, R. Pode, Potential of lithium-ion batteries in renewable energy, Renew. Energy 76 (2015) 375–380, http://dx.doi.org/10.1016/j.renene.2014.11.058.

[4] S.J. Gerssen-Gondelach, A.P.C. Faaij, Performance of batteries for electric vehicles on short and longer term, J. Power Sources 212 (2012) 111–129, http://dx.doi.org/10.1016/J.JPOWSOUR.2012.03.085.

[5] B. Nykvist, M. Nilsson, Rapidly falling costs of battery packs for electric vehicles, Nat. Clim. Change 5 (2015) 329–332, http://dx.doi.org/10.1038/nclimate2564.

[6] J. Wu, X. Xing, X. Liu, J.M. Guerrero, Z. Chen, Energy management strategy for grid-tied microgrids considering the energy storage efficiency, IEEE Trans. Ind. Electron. (2018), http://dx.doi.org/10.1109/TIE.2018.2818660 1–1.

[7] L.Y. Wang, C. Wang, G. Yin, F. Lin, M.P. Polis, C. Zhang, J. Jiang, Balanced control strategies for interconnected heterogeneous battery systems, IEEE Trans. Sustain. Energy 7 (2016) 189–199, http://dx.doi.org/10.1109/TSTE.2015.2487223.

[8] L. Lu, X. Han, J. Li, J. Hua, M. Ouyang, A review on the key issues for lithium-ion battery management in electric vehicles, J. Power Sources 226 (2013) 272–288, http://dx.doi.org/10.1016/j.jpowsour.2012.10.060.

[9] S.M. Rezvanizaniani, Z. Liu, Y. Chen, J. Lee, Review and recent advances in battery health monitoring and prognostics technologies for electric vehicle (EV) safety and mobility, J. Power Sources 256 (2014) 110–124, http://dx.doi.org/10.1016/j.jpowsour.2014.01.085.

[10] X. Gong, R. Xiong, C.C. Mi, Study of the characteristics of battery packs in electric vehicles with parallel-connected lithium-ion battery cells, IEEE Trans. Ind. Appl. 51 (2015) 1872–1879, http://dx.doi.org/10.1109/TIA.2014.2345951.

[11] Y.M. Jeong, Y.K. Cho, J.H. Ahn, S.H. Ryu, B.K. Lee, Enhanced Coulomb counting method with adaptive SOC reset time for estimating OCV, in: 2014 IEEE energy convers, Congr. Expo. ECCE 2014 (2014) 4313–4318, http://dx.doi.org/10.1109/ECCE.2014.6953989.

[12] N. Yang, X. Zhang, G. Li, State of charge estimation for pulse discharge of a LiFePO4 battery by a revised ah counting, Electrochim. Acta 151 (2015) 63–71, http://dx.doi.org/10.1016/j.electacta.2014.11.011.

[13] Y.-S. Lee, M. Liu, C.-C. Sun, M.-W. Cheng, State-of-charge estimation with aging effect and correction for lithium-ion battery, IET Electr. Syst. Transp. 5 (2015) 70–76, http://dx.doi.org/10.1049/iet-est.2013.0007.

[14] Y. Xing, W. He, M. Pecht, K.L. Tsui, State of charge estimation of lithium-ion batteries using the open-circuit voltage at various ambient temperatures, Appl. Energy 113 (2014) 106–115, http://dx.doi.org/10.1016/j.apenergy.2013.07.008.

[15] X. Chen, W. Shen, M. Dai, Z. Cao, J. Jin, A. Kapoor, Robust adaptive sliding-mode observer using RBF neural network for lithium-ion battery state of charge estimation in electric vehicles, IEEE Trans. Veh. Technol. 65 (2016) 1936–1947, http://dx.doi.org/10.1109/TVT.2015.2427659.

[16] M. Shehab El Din, M.F. Abdel-Hafez, A.A. Hussein, Enhancement in Li-Ion battery cell state-of-charge estimation under uncertain model statistics, IEEE Trans. Veh. Technol. 65 (2016) 4608–4618, http://dx.doi.org/10.1109/TVT.2015.2492001.

[17] Z. Chen, Y. Fu, C.C. Mi, State of charge estimation of lithium-ion batteries in electric drive vehicles using extended Kalman filtering, IEEE Trans. Veh. Technol. 62 (2013) 1020–1030, http://dx.doi.org/10.1109/TVT.2012.2235474.

[18] J. Meng, G. Luo, F. Gao, Lithium polymer battery state-of-charge estimation based on adaptive unscented kalman filter and support vector machine, IEEE Trans. Power Electron. 31 (2016) 2226–2238, http://dx.doi.org/10.1109/TPEL.2015.2439578.

[19] J. Chen, Q. Ouyang, C. Xu, H. Su, Neural network-based state of charge observer design for lithium-ion batteries, IEEE Trans. Contr. Syst. Technol. (2017), http://dx.doi.org/10.1109/TCST.2017.2664726.

[20] J.C. Alvarez Anton, P.J. Garcia Nieto, C. Blanco Viejo, J.A. Vilan Vilan, Support vector machines used to estimate the battery state of charge, IEEE Trans. Power Electron. 28 (2013) 5919–5926, http://dx.doi.org/10.1109/TPEL.2013.2243918.

[21] X. Hu, S. Li, Y. Yang, Advanced machine learning approach for lithium-ion battery state estimation in electric vehicles, IEEE Trans. Transp. Electrif 7782 (2015), http://dx.doi.org/10.1109/TTE.2015.2512237 1–1.

[22] G.L. Plett, Extended Kalman filtering for battery management systems of LiPB-based HEV battery packs - Part 3. State and parameter estimation, J. Power Sources 134 (2004) 277–292, http://dx.doi.org/10.1016/j.jpowsour.2004.02.033.

[23] J. Meng, M. Ricco, G. Luo, M. Swierczynski, D.-I. Stroe, A.-I. Stroe, R. Teodorescu,

An overview and comparison of online implementable SOC estimation methods for lithium-ion battery, IEEE Trans. Ind. Appl. 54 (2018) 1583–1591, http://dx.doi.org/10.1109/TIA.2017.2775179.
[24] Z. Chen, Y. Fu, C.C. Mi, State of charge estimation of lithium-ion batteries in electric drive vehicles using extended kalman filtering, Veh. Technol. IEEE Trans. 62 (2013) 1020–1030, http://dx.doi.org/10.1109/TVT.2012.2235474.
[25] Y. Zhang, R. Xiong, H. He, W. Shen, Lithium-ion battery pack state of charge and state of energy estimation algorithms using a hardware-in-the-loop validation, IEEE Trans. Power Electron. 32 (2017) 4421–4431, http://dx.doi.org/10.1109/TPEL.2016.2603229.
[26] X. Liu, Z. Chen, C. Zhang, J. Wu, A novel temperature-compensated model for power Li-ion batteries with dual-particle-filter state of charge estimation, Appl. Energy 123 (2014) 263–272, http://dx.doi.org/10.1016/j.apenergy.2014.02.072.
[27] J. Meng, G. Luo, E. Breaz, F. Gao, A robust battery state-of-charge estimation method for embedded hybrid energy system, IECON 2015-41st Annu. Conf. IEEE Ind. Electron. Soc, 2015, pp. 1205–1210, , http://dx.doi.org/10.1109/IECON.2015.7392264.
[28] M. Cacciato, G. Nobile, G. Scarcella, G. Scelba, Real-time model-based estimation of SOC and SOH for energy storage systems, IEEE Trans. Power Electron. 32 (2017) 794–803, http://dx.doi.org/10.1109/TPEL.2016.2535321.
[29] H. Chaoui, N. Golbon, I. Hmouz, R. Souissi, S. Tahar, Lyapunov-based adaptive state of charge and state of health estimation for lithium-ion batteries, IEEE Trans. Ind. Electron. 62 (2015) 1610–1618, http://dx.doi.org/10.1109/TIE.2014.2341576.
[30] J. Klee Barillas, J. Li, C. Günther, M.A. Danzer, A comparative study and validation of state estimation algorithms for Li-ion batteries in battery management systems, Appl. Energy 155 (2015) 455–462, http://dx.doi.org/10.1016/j.apenergy.2015.05.102.
[31] R. Morello, F. Baronti, X. Tian, T. Chau, R. Di Rienzo, R. Roncella, B. Jeppesen, W.H. Lin, T. Ikushima, R. Saletti, Hardware-in-the-loop simulation of FPGA-based state estimators for electric vehicle batteries, IEEE Int. Symp. Ind. Electron, 2016, pp. 280–285, , http://dx.doi.org/10.1109/ISIE.2016.7744903.
[32] J. Xu, C.C. Mi, B. Cao, J. Deng, Z. Chen, S. Li, The state of charge estimation of lithium-ion batteries based on a proportional-integral observer, IEEE Trans. Veh. Technol. 63 (2014) 1614–1621, http://dx.doi.org/10.1109/TVT.2013.2287375.
[33] X. Tang, Y. Wang, Z. Chen, A method for state-of-charge estimation of LiFePO4 batteries based on a dual-circuit state observer, J. Power Sources 296 (2015) 23–29, http://dx.doi.org/10.1016/j.jpowsour.2015.07.028.
[34] S. Nejad, D.T. Gladwin, D.A. Stone, A systematic review of lumped-parameter equivalent circuit models for real-time estimation of lithium-ion battery states, J. Power Sources 316 (2016) 183–196, http://dx.doi.org/10.1016/j.jpowsour.2016.03.042.
[35] G.L. Plett, Battery Management Systems, Volume Ii: Equivalent-circuit Methods, Artech House Publishers, 2015.
[36] B. Xia, X. Zhao, R. de Callafon, H. Garnier, T. Nguyen, C. Mi, Accurate lithium-ion battery parameter estimation with continuous-time system identification methods, Appl. Energy 179 (2016) 426–436, http://dx.doi.org/10.1016/j.apenergy.2016.07.005.
[37] Y. Hu, Y. Wang, Two time-scaled battery model identification with application to battery state estimation, IEEE Trans. Contr. Syst. Technol. 23 (2014), http://dx.doi.org/10.1109/TCST.2014.2358846 1–1.
[38] X. Tang, X. Mao, J. Lin, B. Koch, Li-ion battery parameter estimation for state of charge, Am. Control Conf. (ACC) (2011) 941–946, http://dx.doi.org/10.1109/ACC.2011.5990963 2011.
[39] H. He, X. Zhang, R. Xiong, Y. Xu, H. Guo, Online model-based estimation of state-of-charge and open circuit voltage of lithium-ion batteries in electric vehicles, Energy 39 (2012) 310–318, http://dx.doi.org/10.1016/j.energy.2012.01.009.
[40] Recursive Algorithms for Online Parameter Estimation - MATLAB & Simulink, (n.d.). https://www.mathworks.com/help/ident/ug/recursive-algorithms-for-online-estimation.html#buagqes (accessed October 6, 2017).
[41] D.I. Stroe, M. Swierczynski, S.K. Kær, R. Teodorescu, Degradation behavior of lithium-ion batteries during calendar ageing - the case of the internal resistance increase, IEEE Trans. Ind. Appl. PP (2017) 1, http://dx.doi.org/10.1109/TIA.2017.2756026.
[42] M. Gholizadeh, F.R. Salmasi, Estimation of state of charge, unknown nonlinearities, and state of health of a lithium-ion battery based on a comprehensive unobservable model, IEEE Trans. Ind. Electron. 61 (2014) 1335–1344, http://dx.doi.org/10.1109/TIE.2013.2259779.
[43] P. Malysz, J. Ye, R. Gu, H. Yang, A. Emadi, Battery state-of-power peak current calculation and verification using an asymmetric parameter equivalent circuit model, IEEE Trans. Veh. Technol. 65 (2016) 4512–4522, http://dx.doi.org/10.1109/TVT.2015.2443975.
[44] Transport - UNECE, (n.d.). http://www.unece.org/trans/main/wp29/wp29regs101-120.html (accessed October 4, 2017).
[45] EPA Urban Dynamometer Driving Schedule (UDDS), (n.d.). https://www.epa.gov/emission-standards-reference-guide/epa-urban-dynamometer-driving-schedule-udds (accessed October 4, 2017).
[46] L. Ljung, S. Torsten, Theory and Practice of Recursive Identification, The MIT Press, 1985, http://dx.doi.org/10.1002/oca.4660060109.
[47] L. Ljung, System Identification: Theory for the User, Prentice Hall, 1999, http://dx.doi.org/10.1016/0005-1098(89)90019-8.

Nomenclature

SOC: State of charge
SOH: State of health
Lithium-ion: Li-ion
EKF: Extended Kalman filter
RLS: Recursive least squares
EV: Electrical vehicle
BMS: Battery management system
OCV: Open circuit voltage
PI: Proportional-integral
ECM: Equivalent circuit model
RC: Resistance and capacitance
RMSE: Root mean square error
UDDS: Urban dynamometer driving schedule
NEDC: New European driving cycle
LQ: Linear quadratic
U_t: the terminal voltage of the battery model (V)
U_1: the voltage of the first RC network (V)
U_2: the voltage of the second RC network (V)
I_L: the battery current (A)
R_0: the ohmic resistance (Ω)
R_1: the resistance of the first RC network (Ω)
C_1: the capacitance of the first RC network (F)
R_2: the resistance of the second RC network (Ω)
C_2: the capacitance of the second RC network (F)
f *(SOC):* the OCV-SOC function (−)
e_{soc}: errors from the inaccurate SOC (−)
e_c: errors from the current sensor (A)
e_u: errors from the voltage sensor (V)
e_p: errors from the parameters uncertainty (−)
ΔU: the voltage difference between the output of the battery model and the terminal voltage(V)
ΔU_1: the voltage difference from the current measurement (V)
ΔU_2: the voltage difference from the inaccurate SOC (V)
ΔU_3: the voltage difference from the parameter uncertainty (V)
$U_{measure}$: the measured voltage from sensor (V)
$I_{measure}$: the measured current from sensor (A)
G_I: the gain of the first PI filter for eliminating the current measurement error (A)
$K_{p,I}$: the proportional gain of the first PI filter (−)
$1/T_i$: the integration gain of the first PI filter (−)
$\hat{I}$: the input current of the battery model corrected by the first PI filter (A)
G_u: the gain of the second PI filter for reducing ΔU_2 (−)
$K_{p,U}$: the proportional gain of the second PI filter (−)
$1/T_{i,U}$: the integration gain of the second PI filter (−)
SOC_i: the corrected SOC by the first PI filter (−)
C_n: the battery capacity (Ah)
η: the Coulombic efficiency (−)
$p_1 \sim p_2$: the weight factor of two PI filters (−)
U_a: the voltage of the battery model if ΔU is the input of the first PI filter (V)
U_b: the voltage of the battery model if ΔU is the input of the second PI filter (V)
U: the voltage measurement (V)
$G(s)$: the transfer function of the two RC ECM (−)
$b_1 \sim b_5$: the parameters to be identified in the discretized two RC model (−)
λ: the forgetting factor (−)
$K(k)$: the gain for parameter identification (−)
$P(k)$: the covariance matrix (−)
K_A: the update coefficient (−)
T: the sampling time (s)
$R_{0,EOL}$: the internal resistance at the end of the battery lifespan (Ω)
$R_{0,new}$: the internal resistance of the new battery (Ω)
x_e: he equilibrium point of the system (−)
K_p: the proportional gain of the identical PI structure (−)
K_{bi}: K_{ai} the integration gains of the identical PI structure (−)
$\hat{x}$: the estimated state of the system (−)
$\Delta_{parameter}$: the error bound of the identified parameters (−)
θ_N: the vector including the identified parameters (−)
θ^*: the vector including the expected parameters (−)